Post-Irradiation Examination results for MgO-CERCER Am-bearing fuels irradiated in PHENIX within the frame of the FUTURIX-FTA experiment.

G. Cecilia, F. Delage, J. Lamontagne, L. Loubet

Proceedings of Global 2015
September 20-24, 2015 - Paris (France)
Paper 5059

Post-Irradiation Examination results for MgO-CERCER Am-bearing fuels irradiated in PHENIX within the frame of the FUTURIX-FTA experiment.

G. Cécilia[1], F. Delage[2], J. Lamontagne[1], L. Loubet[1],
CEA/DEN/DEC, Cadarache Centre, Fuel Study Department, Bt 315, 13108 St Paul Les Durance, France
[1]SA3C; [2]SESC
Tel:+33 442 256 182, Fax: +33 442 257 042, Email:fabienne.delage@cea.fr

Abstract – *The FUTURIX/FTA experiment has been an international program partly implemented within the frame of the FP-6 EUROTRANS and FP-7 FAIRFUELS projects, to demonstrate the technical feasibility, with regard to fuel behaviour of transmuting minor actinides in Accelerator Driven Systems and Fast neutron Reactors dedicated to Minor Actinides burning. 8 Am-bearing fuel compositions: 2 metallic, 2 nitride, 2 Mo-CERMET and 2 MgO-CERCER fuel types with Am contents ranging from 0.2 to 1.9 g.cm^{-3} have been investigated. The MgO-CERCER fuels made of (Pu,Am)O_{2-x} particles dispersed in a magnesia matrix were irradiated in the PHENIX sodium cooled fast reactor up to 6 and 9 at%, at maximum Linear Heat Rates of 80-100W.cm^{-1}. After a recap of the MgO-CERCER fuel pins features as well as the irradiation conditions, the paper gives an overview of the Post Irradiation Examination results gained within the FAIRFUELS European project, on these 2 ADS type fuels. The Post Irradiation Examinations have been performed at the LECA-STAR facility (CEA Cadarache site). Non Destructive Examinations consisted of visual inspections, metrology and gamma spectrometry of pins. Destructive examinations included pin puncturing and released gas analysis, measurements of geometrical and hydrostatic densities of pellets.*

I. INTRODUCTION

Fuels to be used in Accelerator Driven Systems dedicated to Minor Actinides transmutation can be described as highly innovative in comparison with driver fuels of critical Fast neutron Reactors. Indeed, ADS fuels are not fertile, so as to improve the transmutation performance and they contain high volumetric concentrations of minor actinides and plutonium compounds. This unusual fuel composition results in possible degraded performances under irradiation.

A collaborative project (2004-2009) implemented between CEA, JRC-ITU, US/DOE and JAEA made possible to test the irradiation behaviour of a wide range of conceptual Am-bearing fuels for ADS: metallic, nitride, CERamic-METallic and CERamic-CERamic, as well as low fertile fuels for burner Fast Reactor (see Table I). The so-called FUTURIX-FTA test aims at comparing the behaviour of these fuels under similar irradiation conditions in the PHENIX reactor [1]. Part of the programme (dealing with CERMET and CERCER fuels) was performed under the umbrella of the European project FP-6 EUROTRANS [2]. Post irradiation examinations on CERCER and CERMET fuels have been implemented within the FP-7 FAIRFUELS European project [3].

The paper focusses on the irradiation behaviour of the MgO-CERCER fuels that has been investigated by CEA.

The fuels and pins features as well as the irradiation conditions are firstly summarised. Results related to the Non Destructive Examination step (visual inspections, metrology and gamma spectrometry of pins) are then described. Results of pin puncturing and released gas analysis follow. Outcomes from the pellets recovery stage are then presented. Finally fuel pellets metrology and hydrostatic density measurements are given.

TABLE I
FUTURIX-FTA fuel compositions

Pin ID	Composition	Am(g.cm^{-3})
DOE-1	35U29Pu4Am2Np30Zr (wt%)	0.5
DOE-2	48Pu12Am40Zr (wt%)	1.2
DOE-3	$U_{0.50}Pu_{0.25}Am_{0.15}Np_{0.10}N$	1.7
DOE-4	$Pu_{0.2}Am_{0.2}Zr_{0.6}N$	2.7
ITU-5	$Pu_{0.8}Am_{0.2}O_{1.90}$ + 86 vol% Mo	0.3
ITU-6	$Pu_{0.23}Am_{0.25}Zr_{0.52}O_{1.79}$ + 60 vol% Mo	1.0
CEA-7	$Pu_{0.5}Am_{0.5}O_{1.88}$ + 80 vol% MgO	1.0
CEA-8	$Pu_{0.2}Am_{0.8}O_{1.73}$ + 75 vol% MgO	2.0

II. FEATURES OF MGO-CERCER FUELS, PINS AND IRRADIATION CONDITIONS

MgO-CERCER fuel pellets were prepared in shielded cells of the ATALANTE facility in two steps. $(Pu,Am)O_{2-x}$ particles were synthesized oxalic co-conversion. Dense pellets of $(Pu,Am)O_{2-x}$ particles dispersed in an inert magnesia matrix were then prepared using a conventional powder metallurgy process [4]. Characterization results of the sintered pellets CEA-7 and CEA-8 are given in Table II. Fuels microstructures are presented in Figure 1.

TABLE II
MgO-CERCER fuels features [4]

Fuel ID	CEA-7	CEA-8
Pu content (wt%)	19.9	9.1
Am content (wt%)	19.6	35.6
MgO content (wt%)	32.8	28.8
Diameter (mm)	5.19	~5.14
Height (mm)	6.66	6.49
Density ($g.cm^{-3}$)	4.88	5.12
Total porosity (%)	4.5	7.5
Open porosity (%)	0.3*	0.4*
O/M	1.88	1.73
Particles size (µm)	<50	<50
Particle fraction	20 (volume %)	20 (volume %)

*estimation

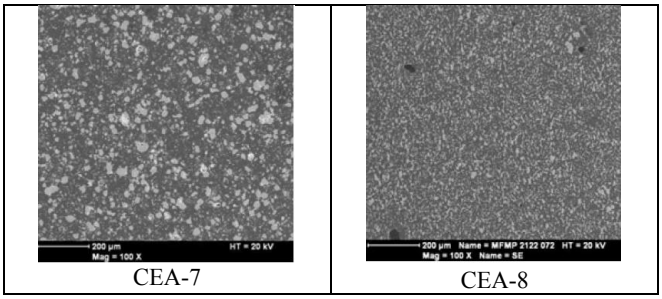

CEA-7 CEA-8

Fig. 1. Scanning Electron Microscope pictures of MgO-CERCER pellets microstructure

The drawing of the pins (the same for both pins) is detailed in Fig. 2. Each pin has got a standard PHENIX diameter and size and is composed of one segment containing the useful stack onto which an extension was welded. Each 100mm CERCER experimental column was centered on the Medium Plane of the Core (MPC) of the reactor core. Each helium-bonded pin included 15 CERCER pellets with such a diameter that the pellet/cladding gap was about 200µm. Three UO_2 pellets with 7% ^{235}U enrichment were positioned on both sides of the CERCER columns to detect cladding failure through the delayed neutron detection system of the reactor. Thermal and chemical insulating hollowed pellets made of MgO and F17 steel respectively, surrounded the CERCER and UO_2 columns. Plena (of $18.6cm^3$) arranged in the experimental segments were filled of helium U (He+Xe:99.995%, O_2<5ppm, N_2<20ppm, H_2O<5ppm) and the initial gas pressure was around 0.1 MPa (at 20 °C).

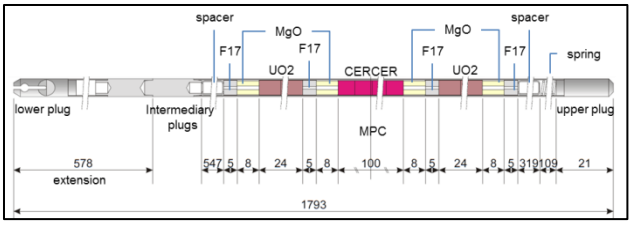

Fig. 2. CERCER pins drawing

The two CERCER pins were positioned in an experimental capsule KCI which also contained 17 standard fuel pins and the DCC-2 carrier containing the KCI capsule was loaded in the PHENIX core (see location in figure 3) between May 2007 and March 2009, i.e. during 235 Equivalent Full Power Days.

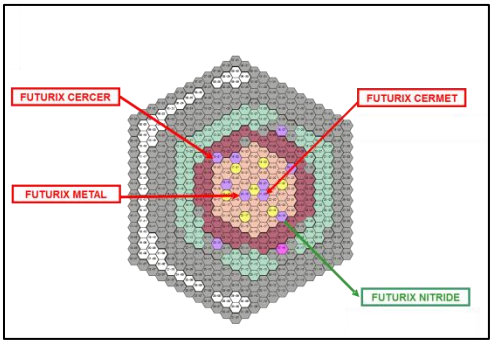

Fig. 3.Location of FUTURIX-FTA pins in the PHENIX core

According to calculations, CERCER pins integrated a cumulative neutron fluence of $9.33x10^{26}n.m^{-2}$. The integrated dose at the maximum flux plane was of 28.69dpa. Calculated burnups were of 8.6at% (i.e. 160 $GWj.m^{-3}$) and 5.75at% (i.e. 133 $GWj.m^{-3}$) for CEA-7 and CEA-8 respectively. Am transmutation rates were of 17.6at% and 19.8at% respectively. Finally, maximum Linear Heat Rates (see figure 4) were within the range: 82-96$W.cm^{-1}$ and 82-87$W.cm^{-1}$ for CEA-7 and CEA-8 respectively.

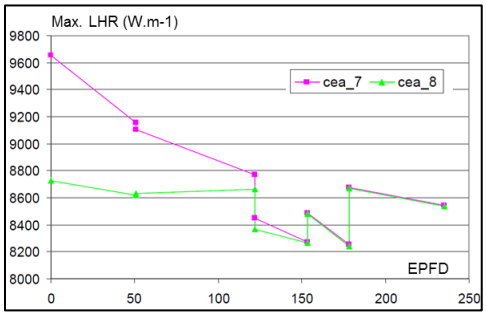

Fig. 4. Maximum Linear Heat Rates versus Equivalent Full power Days of irradiation for CEA-7 and CEA-8 pins

Remark: Thermal calculations performed at the experiment design stage have shown that peak temperatures in nominal irradiation conditions (104 and 87W.cm^{-1} targeted for respectively CEA-7 and CEA-8) would reach 1430°C and 1270°C respectively (subject to assumptions: 10% volume fuel swelling, 50% gas release rate in the pins and 50% MgO thermal conductivity degradation, at the end of irradiation).

III. NON DESTRUCTIVE EXAMINATIONS

Pins metrology measurements were performed in the LECA facility (CEA Cadarache site) on the VENDAUM bench [5] that has been designed to host cylindrical objects of lengths up to 2.7 m with diameters ranging from 6.55 mm (PHENIX pin standard diameters) to 40 mm. The pin held in a vertical position through a mandrel is moved downwards and measurement cartridges are immobile.

The pins CEA-7 and CEA-8 were positioned upright with their base on the bench. The axial reference point was the base of the pin.

Results for pins lengths are given in Table III: As the accuracy of the irradiated pin length is estimated to be ±1 mm at 2σ compared with ±3mm for fabrication, there is no significant elongation for both pins.

TABLE III
Length measurement results

Pins ID	CEA 7	CEA 8
before irradiation	1793 mm	1793 mm
after irradiation	1792.2 mm	1792.0 mm
change	Non-significant	Non-significant

Diameters were measured according to several generatrices. As only the experimental segments are of interest, measurements started at the elevation of 500 mm (i.e. below the connection between the experimental segment and the bottom extension expected at 578 mm from the base).

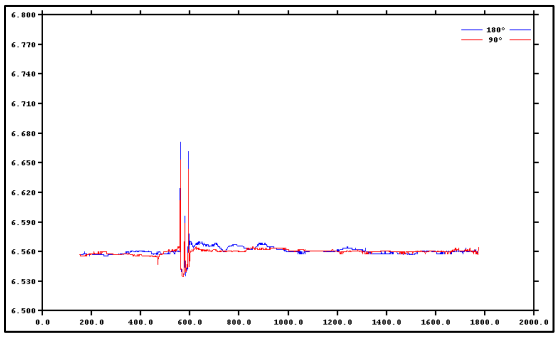

Fig. 5. Diametric measurement of pin CEA 7 according generatrices : 0° (180°) and 90°

Results systematically point out strong variations centered at 578 mm from the base of the pin that corresponds to the intermediary plugs welding area (see figure 5). Outside this area, diameters changes are almost inexistent: deformations at core mid-height plane corresponding to the middle of the experimental column (1243 mm from the base) are of 0.2 and 0.1% for pins CEA-7 and CEA-8 respectively.

Spectrometry measurements of the pins were performed using a numerous isotopes to cover a wide range of spectra. Due to the half-life of some of the isotopes, their counting statistics proved insufficient to allow their analysis. Therefore, instead of the usual 10s of counting per spectrum, data acquisitions lasted 80s. These acquisitions were performed at the usual pitch of 0.5 mm in the area of interest of the pin i.e. from 1200 to 1800mm from the base. In order to obtain a full picture of the flux on these pins, refined measurements of the central part were added with acquisitions of the same time length (80 s) per spectrum for the lower part of the two pins using a less refined pitch. Therefore the "reference" distributions given hereafter show a combination of acquisitions obtained with a mean pitch up to 1000 mm from the base and acquisitions obtained with a refined pitch of 0.5 mm above this point. The lower part must not be considered with the same level of detail and is only given to provide an overall idea of the flux involved.

The axial distributions of the main isotopes used to identify the different components of the pins are presented hereafter: ^{137}Cs for the fuel, ^{60}Co for the steel components and ^{54}Mn for the flux. The figure 6, gathers the results for pin CEA-7 compared to a sketch of the components of the full pin at the same scale so as to visualize the location of the different areas of the pin.

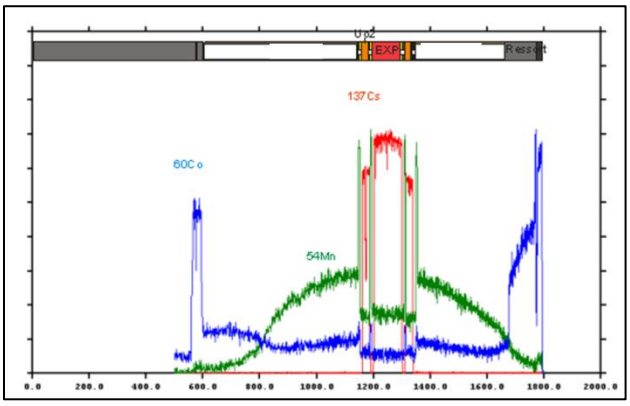

Fig. 6. Superposition of ^{137}Cs, ^{54}Mn and ^{60}Co spectra for pin CEA-7

The area that corresponds to intermediary plugs can be identified thanks to the ^{60}Co signal that increases in the area around the elevation of 578 mm from the base. The plotted line of this isotope also reveals the presence of the

spring in the upper part of the pin. The distribution of ^{54}Mn – an activation element of ^{54}Fe in a fast flux – makes possible to locate the different internal structural components of the pins: the presence of spacers and F17 steel pellets on each side of the experimental column results in a much higher counting rate than in the part containing the experimental pellets (iron-free) for which the ^{54}Mn signal is due to the cladding material only. The distribution of ^{54}Mn makes possible to determine the axial fast neutron flux profile in the experimental column too: this leads to the generally convex appearance of the flux curve (placed near the experimental area indicated above). Finally, the ^{137}Cs profile makes possible to distinguish two UO_2 pellet areas on each side of the central fuel column.

A zoom on the central experimental area (measured with a pitch of 0.5 mm) to refine the corresponding analyses, makes possible to locate all the components and return a good agreement with the manufacturing data (see figures 7 and 8 for CEA-7 and CEA-8 respectively). It can be seen that the F17 spacers (in grey) provoke a rise in ^{60}Co and ^{54}Mn signals. The MgO spacers (in yellow) are not visible in these distributions. The UO_2 pellet areas (in orange) appear in the ^{137}Cs counting on each side of the central experimental column (in red).

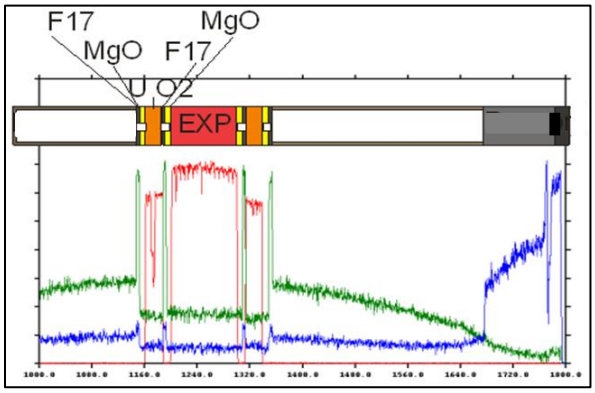

Fig. 6 : Superposition of ^{137}Cs (red), ^{54}Mn (green) and ^{60}Co (blue) spectra for the fuel area in pin CEA-7

It has therefore been possible to determine the lengths of these fuel areas for the two pins and to compare them to results before irradiation (see Table IV). The elongation in the columns of both pins was low (below 1%). As the accuracy of the irradiated fuel column length was estimated at ±1 mm, there is no significant difference in the elongation of the experimental columns between the two pins.

Furthermore, in terms of migration, the usual indication of ^{137}Cs migration is an overall difference in the appearance between the distribution of ^{137}Cs and that of ^{154}Eu (for example), with a rise in the counting rate of ^{137}Cs at the end of the column. In the central area of the two FUTURIX pins, the ^{137}Cs and ^{154}Eu distributions (Figures 8 & 9) both tend to have flat profiles without any rise in the ^{137}Cs counting rate, which leads to conclude that there is no significant migration of this isotope in the pins.

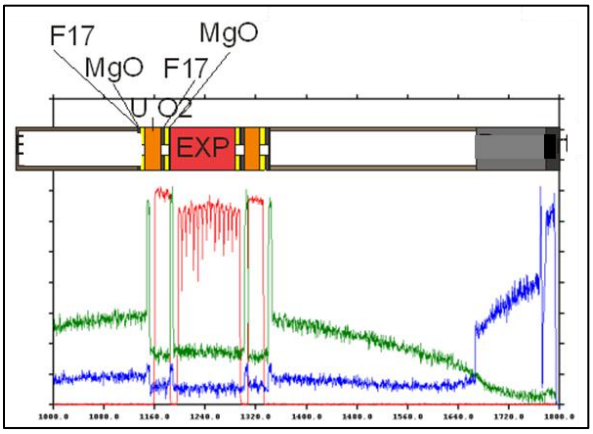

Fig. 7. Superposition of ^{137}Cs (red), ^{54}Mn (green) and ^{60}Co (blue) spectra for the fuel area in pin CEA-8

TABLE IV
Elongation of UO_2 and CERCER fuel stacks

Pins ID	CEA-7	CEA-8
UO_2 lower stack length (mm)		
- before irradiation	24.313	24.478
- after irradiation	27.1*	24.7
UO_2 upper stack length (mm):		
- before irradiation	24.853	24.489
- after irradiation	24.6	24.6
CERCER fuel stack length (mm):		
- before irradiation	99.21	97.35
- after irradiation	100.1	98
→ elongation	0.9%	0.7%

* inter-pellet gap observed

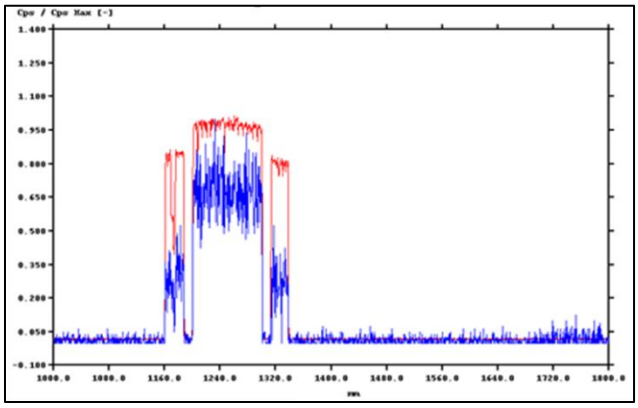

Fig. 8. Comparison between ^{137}Cs (red) and ^{154}Eu (blue) spectra for pin CEA-7

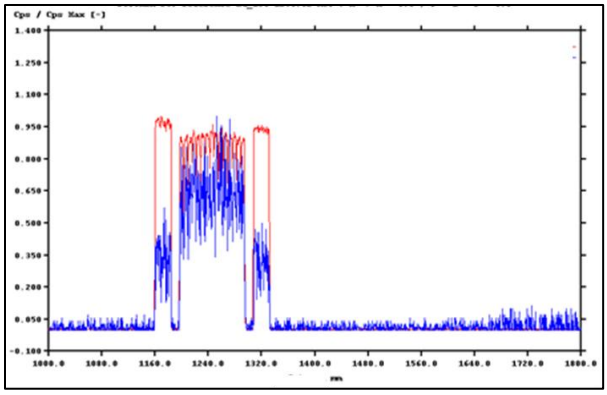

Fig. 8. Comparison between ^{137}Cs (red) and ^{154}Eu (blue) spectra for pin CEA-8

When comparing the ^{137}Cs distributions for the 2 pins pins (see Figure 9), the first noticeable aspect - as already mentioned - is the extremely open inter-pellet space between the first and the second pellet in the lower UO_2 column of the pin CEA-7, which leads to an overestimated elongation of the whole column. Thus, the second pellet in this low column would be damaged. Furthermore, the inter-pellet gaps are clearly much more reduced for pin CEA-8 than for pin CEA-7. In principle, this difference cannot be explained by the differences in the initial geometry of the pellets. So it would be interesting to investigate this point in details. Lastly, by comparing the counting rate of the two UO_2 areas with that of the central experimental area, the counting rates of ^{137}Cs in the UO_2 areas are similar in both pins which seem to indicate similar fabrication, irradiation conditions and behaviour in these areas. However, the ^{137}Cs counting rate in the central area is clearly higher in pin CEA-7 than in CEA-8. This difference is consistent with fuel composition and burnup differences in these areas.

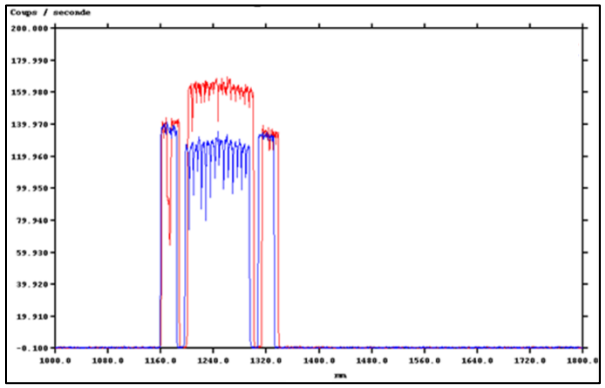

Fig. 9. Comparison of the ^{137}Cs distribution between pins CEA-7 (blue) and CEA-8 (red)

IV. PINS PUNCTURING RESULTS

Pins puncturing were performed at STAR facility (CEA Cadarache site) on a setup designed to investigate small volumes of gas. The puncturing method is based on a static pressure measurement during a double expansion of internal gas in a calibrated capacity. Through the two equilibrium pressures measured, two parameters become available: the final pressure (Pf) and the collected gas volume (Vg) calculated at T=20°C and P=101325Pa. After the puncturing operation, the pin is pumped to high vacuum overnight. Then a known amount of gas is decompressed into the pin and the operation is repeated five times. Using these new equilibriums of pressure, the final free volume (Vf) - i.e. volume of the pin occupied by gas at the end of irradiation - is determined.

Pressure changes during the CEA-7 pin puncturing operation are given in figure 10 for illustration. Results related to the two pins, gathered in Table V, underline that the final pressures and final volumes are quite similar to the initial pressures (0.11MPa) and plena (18.6cm^3), which suggests that very low gas release rates.

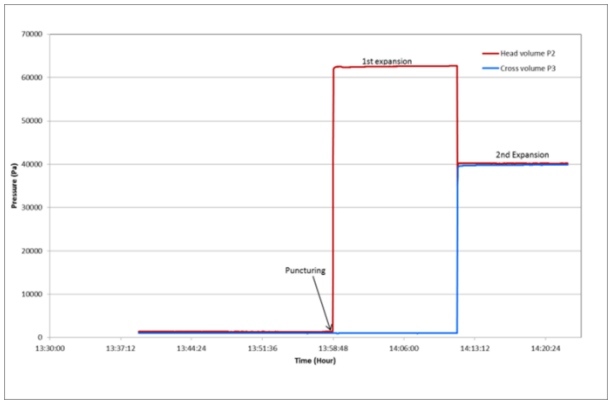

Fig. 10. Pressure build-up results for CEA-7 pin puncturing.

TABLE V
Puncturing results for CEA-7 and CEA-8 pins

Pin ID	CEA-7	CEA-8
Puncturing date	03/02/2014	07/02/2014
Pf (MPa)	0.106±0.015	0.118±0.016
Vg (cm^3)	19.9±4.4	22.3±4.9
Vf (cm^3)	18.9±3.1	18.9±3.2

Remark: uncertainties are calculated in quadratic sum.

Gas collected were analysed by mass spectrometry to determine their chemical and isotopic compositions. Results of gaseous species compositions presented in Table VI point out that helium (initial filling gas of the pins as well as main gas created within the ^{241}Am transmutation scheme) is the highly major species (~99%) in both cases. Isotopic compositions of the fission gases Xe and Kr given

in Table VII and VIII respectively are almost consistent with neutronic calculation results (figures in italic, within Table VII and VIII) performed with the code CESAR.

TABLE VI
Elemental composition of the collected gases

Pin	CEA-7	CEA-8
% H_2	0.002	0.002
% He	98.942	99.336
% Xe	0.466	0.100
% Kr	0.033	0.008
% O_2	0.102	0.065
% N_2	0.425	0.330
% Ar	0.024	0.154
% CO_2	0.006	0.005

TABLE VII
Isotopic composition of Xe for CEA-7 and CEA-8 after irradiation

ID		^{128}Xe	^{130}Xe	^{131}Xe	^{132}Xe	^{134}Xe	^{136}Xe
CEA-7	exp	0.04	0.15	15.89	22.64	31.55	29.73
	calc	*0.04*	*0.08*	*15.95*	*21.65*	*31.98*	*29.98*
CEA-8	exp	0.04	0.16	16.13	22.44	31.98	29.24
	calc	*0.04*	*0.08*	*15.96*	*21.67*	*31.90*	*29.94*

TABLE VIII
Isotopic composition of Kr for CEA-7 and CEA-8 after irradiation

ID		^{82}Kr	^{83}Kr	^{84}Kr	^{85}Kr	^{86}Kr
CEA-7	exp	0.20	19.32	29.40	5.68	45.40
	calc	*0.12*	*16.22*	*28.13*	*6.31*	*49.23*
CEA-8	exp	0.16	18.16	29.01	5.16	47.51
	calc	*0.12*	*15.81*	*27.54*	*6.47*	*50.06*

As the initial volume of gas (assimilated to pure He) filling the pins has been estimated at 20.5 cm^3 (at 20°C and 0.1MPa), maximum volumes of gas released into the pins would be of 3.8cm^3 and 6.7cm^3, for CEA-7 and CEA-8 respectively. Considering calculated quantities of helium and fission gas created in both CERCER and UO_2 fuels up to the time of puncturing (given in table IX), maximum helium fractions released would be of 13% and 12% for CEA-7 and CEA-8 respectively; maximum Kr+Xe fraction released would be less than 0.1% in the 2 cases.

TABLE IX
Calculated results regarding helium and fission gas quantities created in CEA-7 and CEA-8 up to puncturing

gas	CEA-7(moles)	CEA-8 (moles)
He	$1.20x10^{-03}$	$2.32\ x10^{-03}$
Xe	$5.04\ x10^{-04}$	$4.25\ x10^{-04}$
Kr	$4.93\ x10^{-05}$	$4.42\ x10^{-05}$

These results are a bit surprising as the centre fuel pellets temperatures were expected to be higher than 1000°C. Indeed, PIE of the ECRIX H irradiation experiment, pointed out that He and Fission Gas releases were of 23 and 4% respectively, for an Am-bearing MgO CERCER dense fuel (Am content: 0.7g.cm^{-3}) made of $AmO_{1.63}$ particles microdispersed in a MgO matrix, which was irradiated in PHENIX at a maximum temperature of 900°C up to a fission rate of 25at% (i.e.154GWd.m^{-3}) [6].

Microanalysis of the fuels to be done using EPMA and SIMS tools are expected to give the complementary experimental data to confirm the FUTURIX-FTA puncturing results.

V. PELLETS RECOVERY

After the pins were cut at the level of the spacer tube on one side and of the crimped spacer on the other side, pellets of the useful segments were recovered one by one, pushing them out using a metal rod adapted to the internal pins diameter. This operation was easily done, which was indicative of loose pellets. This result is consistent with Non Destructive Examinations that didn't evidenced cladding deformation along the fuel columns.

For the two pins, all MgO hollow pellets (four per pin) are intact and the gap between the pellets and the cladding remain wide (see figure 11a). All F17 spacers (four hollow pellets in each pin) were also recovered in one piece (see figure 11b as an illustration). As represented in figure 12, UO_2 pellets were extracted in several fragments for the two pins. Concerning CERCER fuels, 8 pellets out of 15 were recovered in one piece from the pin CEA-7 (see figure 13a), and 5 pellets out of 15 from the pin CEA-8; the others were extracted in relatively large fragments (figure 13b). All recovered MgO matrix pellets and fragments have been stored in argon inerted containers to prevent MgO degradation by humidity.

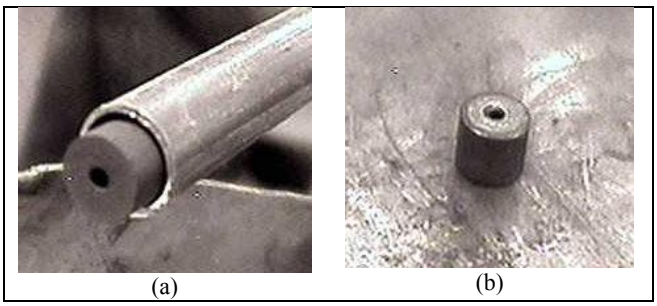

Fig. 11: Pictures of a MgO pellet being extracted (a) and of a F17 spacer (b), from pin CEA-8.

Fig. 12: Illustration of some UO_2 fragments pellet being extracted from pin CEA 7

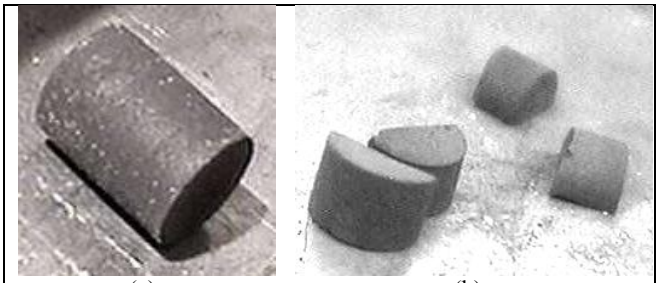

(a) (b)

Fig. 13: Illustration of shapes for extracted Am-bearing CERCER fuels from CEA-7

VI. PELLET METROLOGY AND HYDROSTASTIC DENSITY

Post-irradiation dimensional variations of the Am-bearing fuel pellets recovered in one piece are provided in Table X. Data were obtained by palmer measurements for heights and laser measurements for diameters.

Results outline a low height increase: between 0.6 % and 1.2 % for CEA-7, and between 0.3 % and 1.1 % for CEA-8. The average height increase of 0.8 % for the two pins is consistent with the NDE results that revealed an elongation of the CERCER fuel column around 0.9 % and 0.7 %, or CEA-7 and CEA-8 respectively (see Table IV).

Diameter changes that range between 0.9 and 1.5% for CEA-7, between 0.7 % and 1.5 % for CEA-8. As Diameter and height variation rates are of the same order of magnitude, the CERCER fuel swelling is isotropic. Moreover due to a steady flux profile along the americium-based column of each pin, demonstrated by the ^{137}Cs and ^{154}Eu gamma spectrometry profiles (see section III), there is no significant dimensional variation dispersion among the CERCER fuels. Finally, the dimensional variations are almost the same for CEA-7 and CEA-8.

The geometrical density decreases range from 2.5 % to 3.6 % for CEA-7, and from 2.2 % to 3.5 % for CEA-8. So, the average decrease in the geometrical density is 3.2 % and 3.1 % respectively for CEA-7 and CEA-8. Thus, there is no significant difference between the two fuel compositions. For comparative purposes, the variation in the geometrical density of americium-based targets from the ECRIX-H experiment was of around 6.7 % [7].

Hydrostatic density measurements were performed on three pellets, two from pin CEA-7 and one from pin CEA-8, using the bromobenzene immersion technique. Hydrostatic density results are presented in Table XI. The results reveal no significant post-irradiation de-densification of the fuels. The geometrical density variations are greater than the hydrostatic density variations. The difference can be explained by the fact that hydrostatic density makes it possible to disregard the surface defects on the targets and also does not account for any open porosity that can be formed during the irradiation.

TABLE X
Dimensional variations of CERCER fuels after irradiation

Target #	Δ Height (%)	Δ Diameter (%)	Δ Geometrical density (%)
Futurix FTA 7			
5114	**0,7**	**1,5**	**-3,6**
5119	**0,6**	**1,3**	**-3,1**
5120	**0,6**	**1,5**	**-3,4**
5121	**1,2**	**1,2**	**-3,6**
5126	**0,8**	**1,3**	**-3,3**
5127	**0,7**	**0,9**	**-2,5**
5128	**0,9**	**1,3**	**-3,4**
5129	**0,7**	**1,1**	**-2,8**
Futurix FTA 8			
2112	**1,1**	**1,1**	**-3,2**
2113	**0,9**	**1,2**	**-3,2**
2117	**0,7**	**1,4**	**-3,5**
2124	**0,8**	**0,7**	**-2,2**
2120	**0,3**	**1,5**	**-3,2**

TABLE XI
Hydrostatic density measurements

Target #	Hydrostatic density ($g.cm^{-3}$)		Δ Hydrostatic density (%)
	Fresh	Irradiated	
Futurix FTA 7			
5119	4,86	4,84	**-0,4**
5129	4,84	4,83	**-0,2**
Futurix FTA 8			
2112	5,21	5,19	**-0,4**

VII. CONCLUSION

Am-bearing driver fuels for Accelerator Driven Systems are highly innovative in comparison with those that could be used for Am-transmutation in Sodium Fast Reactor: they would not be fertile so as to improve the Am

transmutation performance, and they would contain high volumetric contents (~50%) of both Am and Pu oxides diluted in an Inert Matrix. Even if the irradiation behaviour of these innovative fuels remains quite unknown, major roles from irradiation conditions (including temperature), helium production and material swelling due to microstructure modifications, amorphization, helium accumulation..., are expected. The FUTURIX-FTA experiment aims at investigating the irradiation behaviour of a wide range of Am-bearing fuels (metallic, nitride, MgO-CERCER and Mo-CERMET) within the frame of an international collaboration. This paper has focused on the first Post Irradiation Examinations performed on the 2 Am-bearing MgO-CERCER fuels that were irradiated in the PHENIX reactor during 235 EFPD. The initial compositions of the fuels were: $Pu_{0.5}Am_{0.5}O_{1.88}$ + 80vol% MgO and $Pu_{0.2}Am_{0.8}O_{1.73}$ + 75vol% MgO, for pin CEA-7 and pin CEA-8 respectively.

The pins CEA7 and CEA8 were firstly the subject of several specific Non-Destructive Examinations: length, diameter and gamma spectrometry measurements and promising results were obtained for the two pins. The two pins experienced non-significant elongations and deformations. No sign of global ^{137}Cs migration was detected too. One main difference between the pins, was related to the different ^{137}Cs profiles in the gamma scanning analysis for the experimental fuel stacks, with a higher counting rate for CEA-7, that is nevertheless consistent with the expected fission rates.

Pins puncturing and gas analysis were performed too. The amounts of helium and fission gases created in the fuels, that released in the pins were very low in both pins. Helium maximum release rates were of 11-12% in both cases. Xe+Kr maximum release rates were of 1.4% for CEA-7 and 0.6% for CEA-8. These results are a bit surprising compared to the ECRIX-H test results [6] as the irradiation temperature in ECRIX-H was lower and the gas release rates higher for the same kind of fuel micro-structure. Microanalysis of the fuels, to be done in a near future using EPMA and SIMS tools, are expected to give the complementary experimental data that will clarify these results.

Regarding fuel pellets recovery and swelling assessments, a significant fraction of Am-bearing CERCER fuel pellets were recovered as one piece and the measurements of their geometrical density have underlined a moderated (~3%) and almost similar swelling for the two fuel compositions. Results of hydrostatic measurements reveal no significant post-irradiation de-densification of the fuels too.

The next step will consist on optical microscopy and microanalysis (SEM, EPMA, …) to investigate changes in the fuel microstructures after irradiation (size of particles, gas retention, particle/matric interfaces, distribution of elemental species, …). These latest Destructive Examinations are expected in order to confirm the very promising behaviour of these fuels.

ACKNOWLEDGMENTS

The authors appreciate the financial support of the European Commission through the grant agreements 516520 (FP6-EUROTRANS) and 232624 (FP-7 FAIRFUELS).

NOMENCLATURE

ADS: Accelerator Driven System
CERCER: CERamic-CERamic
CERMET: CERamic-METallic
DE : Destructive Examinations
EFPD : Equivalent Full Power Days
EPMA: Electron Probe Micro-Analyser
FR : Fast Reactor
NDE : Non Destructive Examinations
PIE: Post Irradiation Examinations
SEM : Scanning Electron Microscopy
SFR: Sodium cooled Fast Reactor
SIMS: Secondary Ions Mass Spectrometry

REFERENCES

1. E. BRUNON et al., “The FUTURIX-FTA experiment in PHENIX”, Proc. of 8-IEMPT (Nov. 9-11, Las Vegas), 335 (2004)
2. J. KNEBEL et al., “Transmutation of high level waste in an accelerator driven system: towards a demonstration device of industrial interest (EUROTRANS)”, Proc. of FISA (June 22-24,Prague), 286 (2009)
3. http://www.fp7-fairfuels.eu/
4. F. JORION et al., “The FUTURIX-FTA experiment in PHENIX: Status of oxides fuels fabrication”, Proc. of GLOBAL’07 (Sept. 9-13, Boise), 1353 (2007)
5. L. LOUBET, “The contribution of the bench VENDAUM in LECA-STAR (Cadarache) for Non Destructive Examinations”, e-proceedings of HotLab (Sept. 23-26, Idaho Falls) (2013)
6. S. BEJAOUI et al., “ECRIX-H experiment – Synthesis of post-irradiation examination and simulations”, Jour. Nuc. Mat. 415, 158 (2011).
7. J. LAMONTAGNE et al., “Swelling under irradiation of MgO pellets containing americium oxide: The ECRIX-H irradiation experiment”, Jour. Nuc. Mat. 413, 137 (2011)